Thermodynamic Study on Phase Transition in Adsorbed Film of Fluoroalkanol at the Hexane/Water Interface. 6. Pressure Effect on the Phase Transition in the Adsorbed Film of Alkanol and Fluoroalkanol Mixture

Takanori Takiue,* Takayuki Toyomasu, Norihiro Ikeda,† and Makoto Aratono

Department of Chemistry, Faculty of Science, Kyushu University 33, Fukuoka 812-8581, Japan

Received: February 4, 1999

The phase transition in the adsorbed film of 1-icosanol ($C_{20}OH$) and 1,1,2,2-tetrahydroheptadecafluorodecanol ($FC_{10}OH$) mixture at the hexane/water interface was studied by measuring the pressure dependence of interfacial tension at a specific composition of $FC_{10}OH$ $X_2 = 0.280$ and 298.15 K and evaluating the volume change of adsorption. By drawing the interfacial pressure π vs mean area per adsorbed molecule A curve, it was clarified that three types of first-order phase transitions (gaseous−expanded, expanded−$FC_{10}OH$ condensed, and FC_{10}-OH condensed−$C_{20}OH$ condensed) take place in the adsorbed film. The phase transition from the $FC_{10}OH$ condensed to the $C_{20}OH$ condensed state was accompanied by a decrease of the volume change associated with adsorption $\Delta\nu$. By evaluating the partial molar volume change of adsorption, $\bar{\nu}_i^{\mathrm{H}}-\nu_i^{\mathrm{O}}$, and comparing its pressure dependence between the $FC_{10}OH$ condensed and $C_{20}OH$ condensed states, it was suggested that the pressure dependence of the partial molar volume is in the order of $\partial\nu_2^{\mathrm{O}}/\partial p > \partial\nu_1^{\mathrm{O}}/\partial p > \partial\bar{\nu}_2^{\mathrm{H}}/\partial p \approx \partial\bar{\nu}_1^{\mathrm{H}}/\partial p$. Furthermore, it was found that the transition pressure π^{eq} of the $FC_{10}OH$ condensed−$C_{20}OH$ condensed transition (second transition) increases and the corresponding one of the expanded−$FC_{10}OH$ condensed transition (first transition) decreases with increasing pressure. This difference was explained by means of the $\bar{\nu}_i^{\mathrm{H}}-\nu_i^{\mathrm{O}}$ values at the phase transition point.

Introduction

Recently, some powerful techniques such as Brewstar angle microscopy[1,2] and grazing incidence X-ray diffraction[3] have been developed for observing the structure of monolayer at the air/water surface. On the other hand, there are few methods to visualize the film structure at the oil/water interface which plays an important role to determine the structures and properties of molecular organized systems such as microemulsions.[4] Thus far, several workers have investigated the adsorption behavior of surface active substances at the oil/water interfaces,[5−9] and we also have studied it by means of the interfacial tension measurement and thermodynamic analysis.[10−13] In our previous studies,[14,15] we have investigated the phase transition in the adsorbed films of long-chain fluorinated alcohols at the hexane/water interface by measuring the pressure dependence of interfacial tension and evaluating the partial molar volume change associated with adsorption. It was found that the adsorbed film of 1,1,2,2-tetrahydroheptadecafluorodecanol ($FC_{10}OH$) exhibits two types of phase transitions from the gaseous to the expanded state and from the expanded to the condensed one and that the adsorbed film of 1,1,2,2-tetrahydrohenicosafluorododecanol ($FC_{12}OH$) exhibits only one transition from the gaseous to the condensed state. By comparing the partial molar volume change of adsorption between the fluorinated and hydrogenated alcohols, it was suggested that the microscopic circumstance in the adsorbed film affects appreciably the volume change of adsorption.[14]

Furthermore, we have studied the phase transition in the adsorbed film of 1-icosanol ($C_{20}OH$) and $FC_{10}OH$ mixture, both of which exhibit the phase transition between the expanded and the condensed states in their pure adsorbed film, by measuring the interfacial tension as a function of total molality m and the composition of $FC_{10}OH$ X_2 at 298.15 K under atmospheric pressure.[16] It was found that all the γ vs m curves have a break point (first break) which corresponds to the phase transition from the expanded to the condensed state and the curves at $X_2 = 0.275$ and 0.280 show another break (second break) at a high concentration. From the thermodynamic analysis, it was concluded that the second break point corresponds to the phase transition from the $FC_{10}OH$ condensed to the $C_{20}OH$ condensed film.

To confirm the above conclusion and then afford a deeper insight into the phase transition, we examined the pressure effect on the phase transition in the adsorbed film of $C_{20}OH$ and FC_{10}-OH mixture at the specific composition $X_2 = 0.280$. The interfacial tension of hexane solution of $C_{20}OH$ and $FC_{10}OH$ mixture of this composition against water was measured as a function of pressure and total molality. The interfacial pressure π vs mean area per adsorbed molecule A curve was drawn and compared with the corresponding curves of pure alcohols. Furthermore, the partial molar volume change of adsorption was evaluated to make clear the type and properties of the phase transition in the adsorbed film found at $X_2 = 0.280$.

* To whom correspondence should be addressed: Takanori Takiue, Department of Chemistry, Faculty of Science, Kyushu University, Hakozaki, Higashi-ku, Fukuoka 812-8581, Japan. E-mail: t.takscc@mbox.nc.kyushu-u.ac.jp.

† Present address: Department of Environmental Science, Faculty of Human Environmental Science, Fukuoka Women's University, Fukuoka 813-8529, Japan.

10.1021/jp990422z CCC: $18.00
Published on Web 07/20/1999

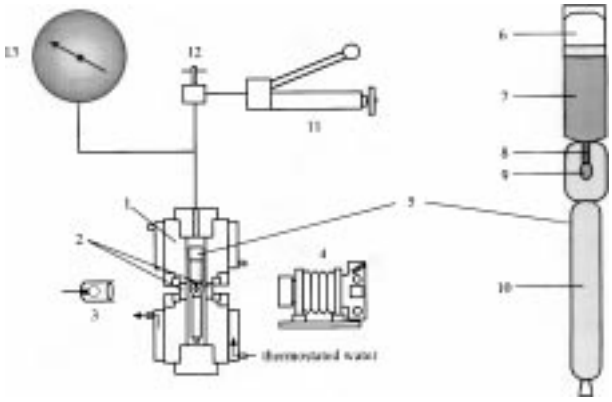

Figure 1. Schematic diagram of the apparatus of the interfacial tension measurement under high pressure: (1) pressure vessel, (2) sapphire window, (3) light source, (4) camera, (5) quartz cell, (6) plunger, (7) syringe, (8) drop forming tip, (9) pendant drop, (10) cylinder, (11) pressure pump, (12) valve, (13) Heise bourdon gauge.

Experimental Section

1-Icosanol ($C_{20}OH$) and 1,1,2,2-tetrahydroheptadecafluorodecanol ($FC_{10}OH$) were purified by the same methods described in the previous papers.[14,16] The interfacial tension γ of the hexane solution of $C_{20}OH$ and $FC_{10}OH$ mixture against water was measured as a function of pressure p and the total molality m at the composition of $FC_{10}OH$ $X_2 = 0.280$ and 298.15 K. Here m and X_2 are defined respectively by

$$m = m_1 + m_2 \tag{1}$$

and

$$X_2 = m_2/m \tag{2}$$

The pendant drop technique[17] was adopted for the interfacial tension measurement under high pressure. In Figure 1 is shown the schematic diagram of the apparatus designed originally in our laboratory.[18] The pressure vessel is a cylinder of chrome−molybdenum steel in which two sapphire windows are equipped to take the picture of the pendant drop profiles by the camera. The measurement cell is made of quartz and consists of plunger, syringe, drop forming tip, and cylinder. The syringe and cylinder are filled with water and hexane solution, respectively. Temperature was kept constant by circulating thermostated water in the jacket around the pressure vessel. Pressure is generated by use of a hand-screw pump and measured with a Heise bourdon gauge. As pressure rises, the pendant drop is formed by the contraction in volumes of water and hexane solution phases. The error in γ value estimated in this study was within 0.05 mN m^{-1}. This value is less than or equal to that achieved by the axisymmetric drop shape analysis based on digitizing the image of the pendant drop.[19−21]

Results and Discussions

The interfacial tension γ measured in this study was plotted against pressure p in Figure 2. It is seen that the γ value increases slightly at very low concentrations and decreases rapidly at high concentrations. The point to be noted is that the γ vs p curve has zero, one, or two break points depending on the total molality. In Figure 3 are plotted the interfacial tension

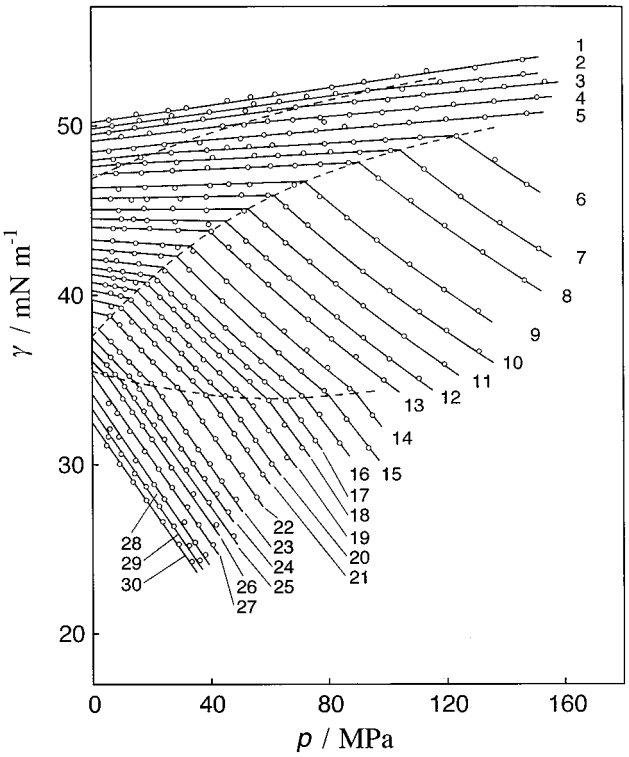

Figure 2. Interfacial tension vs pressure curves at constant total molality and $X_2 = 0.280$: (1) $m = 0$ mmol kg^{-1}, (2) 0.250, (3) 0.500, (4) 1.001, (5) 1.501, (6) 2.002, (7) 2.501, (8) 3.004, (9) 4.002, (10) 4.502, (11) 5.513, (12) 6.267, (13) 7.020, (14) 8.001, (15) 9.000, (16) 10.035, (17) 10.753, (18) 11.549, (19) 12.562, (20) 13.502, (21) 15.501, (22) 16.003, (23) 17.753, (24) 19.002, (25) 20.001, (26) 21.000, (27) 22.501, (28) 24.002, (29) 25.012, (30) 26.001.

γ^{eq} and the total molality m^{eq} at these break points against p. Deducing from our previous finding under atmospheric pressure[16] that the γ vs m curve at $X_2 = 0.280$ has two break points which correspond to the phase transitions from the expanded to the condensed state (called as the first break in ref 16) and from the $FC_{10}OH$ condensed to the $C_{20}OH$ condensed state (the second break) in the adsorbed film, the curves 1 and 2 in Figure 3 correspond to the trajectories of the first and second break points, respectively. Curve 3 designates the trajectory of the break point observed at low concentration and high interfacial tension. It should be noted that the γ^{eq} value of the second break point decreases at low pressures and then increases slightly at high pressures. The γ values read from Figure 2 at a given p were plotted against m in Figure 4: the γ value decreases with increasing m and three break points are observed on the γ vs m curves.

Adopting temperature T, pressure p, total molality m, and composition of $FC_{10}OH$ X_2 as independent variables, the total differential of interfacial tension γ is written as

$$d\gamma = -\Delta s dT + \Delta v d\,p - (\Gamma^H RT/m)dm - (\Gamma^H RT/X_1X_2)(X_2^H - X_2)dX_2 \tag{3}$$

for the system with two nonionic surface-active substances.[22] Here Δy is the thermodynamic quantity change associated with adsorption of solutes given by

$$\Delta y = y^H - \Gamma_1^H y_1^O - \Gamma_2^H y_2^O, \qquad y = s, v \tag{4}$$

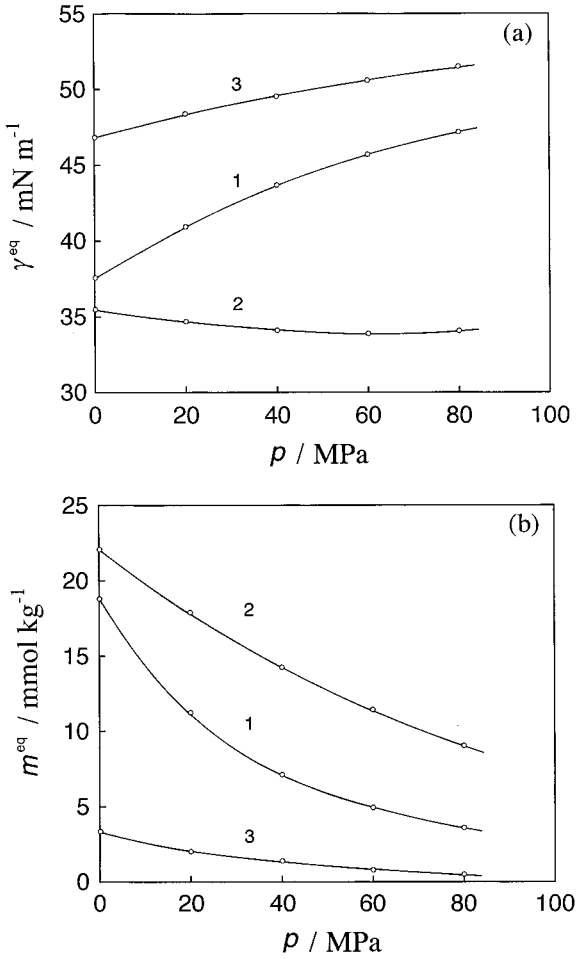

Figure 3. (a) Equilibrium interfacial tension vs pressure curves; (b) equilibrium total molality vs pressure curves: (1) expanded−condensed transition, (2) $FC_{10}OH$ condensed−$C_{20}OH$ condensed transition, (3) gaseous−expanded transition.

and Γ^H and X_2^H are respectively the total interfacial density and the composition of the adsorbed film defined by

$$\Gamma^H = \Gamma_1^H + \Gamma_2^H \tag{5}$$

and

$$X_2^H = \Gamma_2^H/\Gamma^H \tag{6}$$

To make clear the state of the adsorbed film, we first evaluated the total interfacial density Γ^H by applying

$$\Gamma^H = -(m/RT)(\partial\gamma/\partial m)_{T,p,X_2} \tag{7}$$

to the γ vs m curves and then calculated the interfacial pressure π and the mean area per adsorbed molecule A values by using

$$\pi = \gamma^0 - \gamma \tag{8}$$

and

$$A = 1/N_A\Gamma^H \tag{9}$$

respectively, where γ^0 is the interfacial tension of the pure hexane/water interface and N_A is Avogadro's number. The results are shown as the Γ^H vs m and π vs A curves at constant pressure in Figures 5 and 6, respectively. The Γ^H value increases

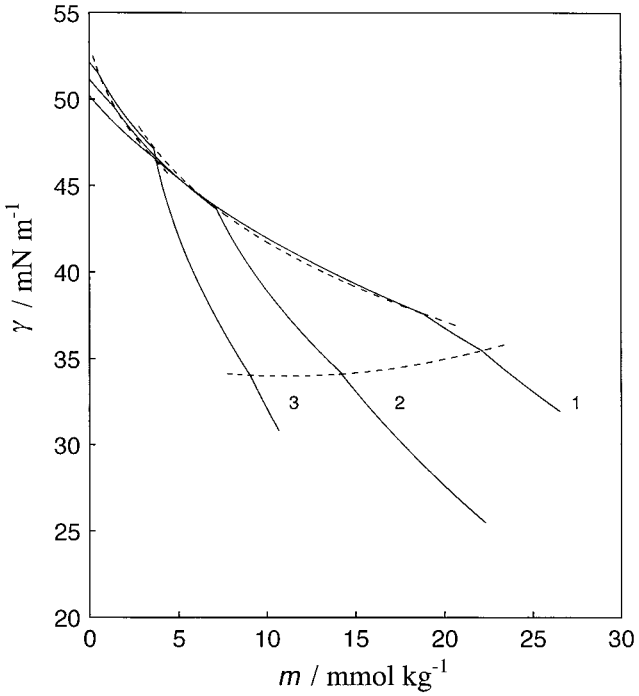

Figure 4. Interfacial tension vs total molality curves at constant pressure: (1) $p = 0.1$ MPa, (2) 40, (3) 80.

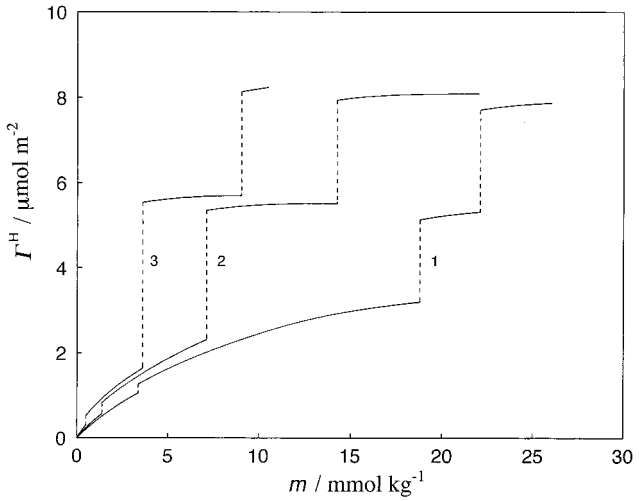

Figure 5. Total interfacial density vs total molality curves at constant pressure: (1) $p = 0.1$ MPa, (2) 40, (3) 80.

with increasing m and changes discontinuously at the phase transition points. Furthermore, it is seen from Figure 6 that the π vs A curves consist of four parts connected by the three discontinuous changes. These results show that there exist four different states in the adsorbed film of $C_{20}OH$ and $FC_{10}OH$ mixture at $X_2 = 0.280$.

These states are identified by comparing the π vs A curve at $X_2 = 0.280$ with those at $X_2 = 0$ ($C_{20}OH$) and 1 ($FC_{10}OH$) at 40 MPa in Figure 7. Taking account of our previous results that the adsorbed film of $FC_{10}OH$ exhibits the three kinds of states (gaseous, expanded, and condensed states) and that of $C_{20}OH$ exhibits two (expanded and condensed states), we realize that the phase transition from the expanded to the $FC_{10}OH$ condensed state takes place at the first break point and from the $FC_{10}OH$ condensed to the $C_{20}OH$ condensed state at the second. This result is totally in accord with our conclusion obtained in the previous studies.[16] Furthermore, we can say that the adsorbed film exhibits also the phase transition between the

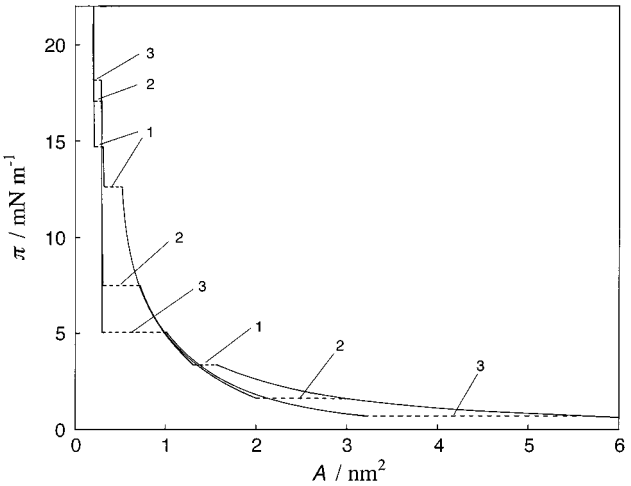

Figure 6. Interfacial pressure vs mean area per adsorbed molecule curves at constant pressure: (1) $p = 0.1$ MPa, (2) 40, (3) 80.

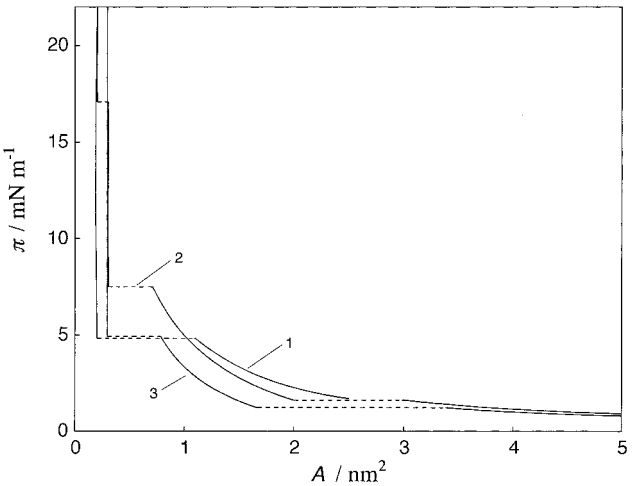

Figure 7. Interfacial pressure vs mean area per adsorbed molecule curves at 40 MPa: (1) $X_2 = 0$ ($C_{20}OH$), (2) 0.280, (3) 1 ($FC_{10}OH$).

gaseous and the expanded states at low concentrations. We should note in Figure 6 that the transition pressure π^{eq} of the second break point increases while that of the first decreases with increasing pressure. This difference will be examined later in this paper.

Next, let us consider the adsorption behavior from the viewpoint of volume. At first, we evaluated the volume change associated with the adsorption $\Delta\nu$ by using

$$\Delta\nu = (\partial\gamma/\partial p)_{T,m,X_2} \tag{10}$$

and plotted its value against m in Figure 8. It is seen that the $\Delta\nu$ value decreases with increasing adsorption and changes discontinuously at the phase transition points. It is positive in the gaseous state and decreases gradually from positive to negative value with increasing concentration in the expanded state. Since the $\Delta\nu$ values of the $C_{20}OH$ condensed state are found to be more negative than that of the $FC_{10}OH$ condensed state, the phase transition from the $FC_{10}OH$ condensed to the $C_{20}OH$ condensed state is accompanied by the large decrease in $\Delta\nu$ value. Furthermore, it should be noted that the $\Delta\nu$ value of the $FC_{10}OH$ condensed state depends strongly on pressure and is very close to the $\Delta\nu$ value of the pure $FC_{10}OH$ system (Figure 6 in ref 14), while that of the $C_{20}OH$ condensed state is practically independent of pressure.

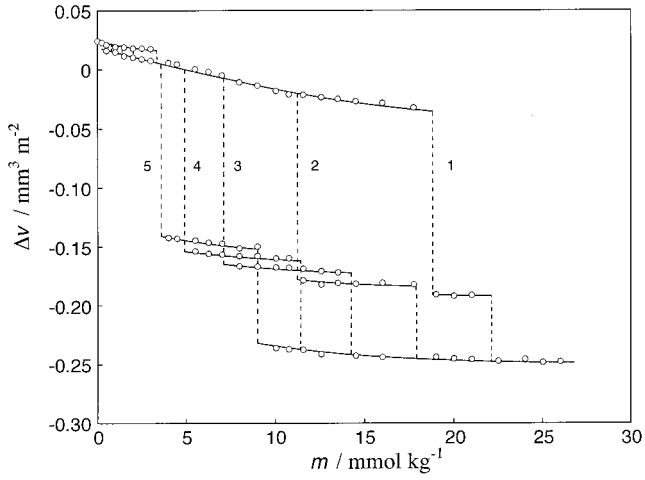

Figure 8. Volume change associated with adsorption vs total molality curves at constant pressure: (1) $p = 0.1$ MPa, (2) 20, (3) 40, (4) 60, (5) 80.

Here we disclose more the significance of $\Delta\nu$ in terms of the partial molar volume change of adsorption of solutes. According to the thermodynamics of adsorption at interfaces,[23] the volume change associated with adsorption is expressed in terms of the partial molar volumes by

$$\Delta\nu = \Gamma_w^I(\bar{\nu}_w^I - \nu_w^W) + \Gamma_o^I(\bar{\nu}_o^I - \nu_o^O) + \Gamma_1^H(\bar{\nu}_1^H - \nu_1^O) + \Gamma_2^H(\bar{\nu}_2^H - \nu_2^O) \tag{11}$$

where $\bar{\nu}_2^H$ is the mean partial molar volume of component i inherent in the interface. The first two terms are responsible for the solvent components (water and hexane) and are negligibly small in the condensed state.[11,14] Considering that the condensed film is constructed by only $C_{20}OH$ or $FC_{10}OH$ molecules,[24] therefore, $\Delta\nu/\Gamma^H$ can be reduced to

$$\Delta\nu/\Gamma^H \approx \bar{\nu}_1^H - \nu_1^O \tag{12}$$

for $C_{20}OH$ condensed film and

$$\Delta\nu/\Gamma^H \approx \bar{\nu}_2^H - \nu_2^O \tag{13}$$

for $FC_{10}OH$ condensed film, respectively. Then $\Delta\nu/\Gamma^H$ corresponds to the partial molar volume change of adsorption of solutes and offers better understanding of $\Delta\nu$ and the difference in pressure dependence of $\Delta\nu$ between the two kinds of condensed films.

The $\Delta\nu/\Gamma^H$ vs m curves are illustrated in the condensed states region at 0.1, 40, and 80 MPa in Figure 9. It is seen that the $\Delta\nu/\Gamma^H$ value is apparently negative: the partial molar volumes of the film forming substances in the adsorbed film are smaller than those in the bulk solution. This is undoubtedly due to the orientation and the restricted thermal motion at the interface. Furthermore, Figure 9 demonstrates that the values of $FC_{10}OH$ condensed state depend more strongly on pressure than those of $C_{20}OH$ condensed state: $\bar{\nu}_1^H - \nu_1^O > \bar{\nu}_2^H - \nu_2^O$ at 0.1MPa and $\bar{\nu}_1^H - \nu_1^O < \bar{\nu}_2^H - \nu_2^O$ at 80 MPa. This result is examined further as follows by introducing the derivative of γ^{eq} at the second break point with respect to p and considering the situation in the condensed film where the hydrocarbon chain of $C_{20}OH$ molecules is surrounded almost by hydrocarbon chains both in the interface and in the solution, while the fluorocarbon chain of $FC_{10}OH$ molecules is surrounded almost by fluorocarbon in the interface but by hydrocarbon in the solution.

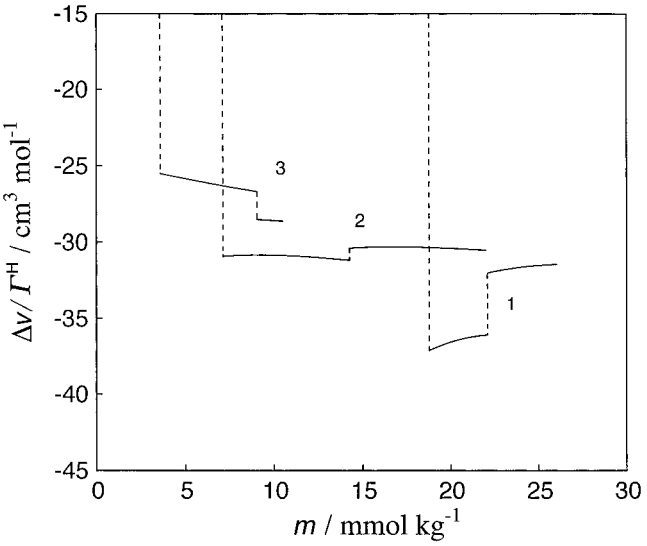

Figure 9. Volume change of adsorption per mole of solutes vs total molality curves at constant pressure: (1) $p = 0.1$ MPa, (2) 40, (3) 80.

When the two states α and β coexist in the interface, eq 3 yields the total differential of γ^{eq} as

$$d\gamma^{eq} = -[(\Delta s^{\beta}/\Gamma^{H,\beta} - \Delta s^{\alpha}/\Gamma^{H,\alpha})/(1/\Gamma^{H,\beta} - 1/\Gamma^{H,\alpha})]dT + [(\Delta v^{\beta}/\Gamma^{H,\beta} - \Delta v^{\alpha}/\Gamma^{H,\alpha})/(1/\Gamma^{H,\beta} - 1/\Gamma^{H,\alpha})]d\,p - [(RT/X_1X_2)(X_2^{H,\beta} - X_2^{H,\alpha})/(1/\Gamma^{H,\beta} - 1/\Gamma^{H,\alpha})]dX_2 \quad (14)$$

Here the states α and β are referred to as the $C_{20}OH$ condensed and $FC_{10}OH$ condensed states, respectively; $\Gamma^{H,\alpha} > \Gamma^{H,\beta}$ at all pressures (see Figure 5). Substituting eqs 12 and 13 into the pressure coefficient of γ^{eq}, we have

$$(\partial\gamma^{eq}/\partial p)_{T,X_2} = [(\bar{v}_2^{H,\beta} - v_2^{O}) - (\bar{v}_1^{H,\alpha} - v_1^{O})]/(1/\Gamma^{H,\beta} - 1/\Gamma^{H,\alpha}) \quad (15)$$

Therefore the negative value of $(\partial\gamma^{eq}/\partial p)_{T,X_2}$ corresponds to the inequality $\bar{v}_1^{H,\alpha} - v_1^{O} > \bar{v}_2^{H,\beta} - v_2^{O}$ and the positive to that $\bar{v}_1^{H,\alpha} - v_1^{O} < \bar{v}_2^{H,\beta} - v_2^{O}$. One should note the correspondence between the curve 2 in Figure 3(a) and the results shown in Figure 9.

Since it is reasonably assumed from Figure 5 that $\Gamma^{H,\alpha}$ and $\Gamma^{H,\beta}$ are almost independent of pressure, the second derivative of γ^{eq} is given in terms of the isothermal pressure coefficients of the partial molar volumes by

$$\partial^2\gamma^{eq}/\partial\, p^2 = [(\partial\bar{v}_2^{H,\beta}/\partial\, p - \partial v_2^{O}/\partial\, p) - (\partial\bar{v}_1^{H,\alpha}/\partial\, p - \partial v_1^{O}/\partial\, p)]/(1/\Gamma^{H,\beta} - 1/\Gamma^{H,\alpha}) \quad (16)$$

Now it is expected that the pressure coefficients of the condensed films are not very dependent on materials and are very small compared to those of the liquid state, $|\partial v_2^{O}/\partial p|$, $|\partial v_1^{O}/\partial p| > |\partial\bar{v}_2^{H,\beta}/\partial p| \approx |\partial\bar{v}_1^{H,\alpha}/\partial p|$, because the condensed film is similar to solid state in the molecular packing. Therefore, the experimental finding that $\partial^2\gamma^{eq}/\partial p^2$ is positive as shown in Figure 3(a) suggests also that the absolute value of $\partial v_2^{O}/\partial p$ is larger than that of $\partial v_1^{O}/\partial p$, i.e., $|\partial v_2^{O}/\partial p| > |\partial v_1^{O}/\partial p| > |\partial\bar{v}_2^{H,\beta}/\partial p| \approx |\partial\bar{v}_1^{H,\alpha}/\partial p|$.

In Figure 6, it has been stated that the π^{eq} of the first break point decreases and that of the second increases with increasing pressure. This is demonstrated more clearly by the π^{eq} vs p plots

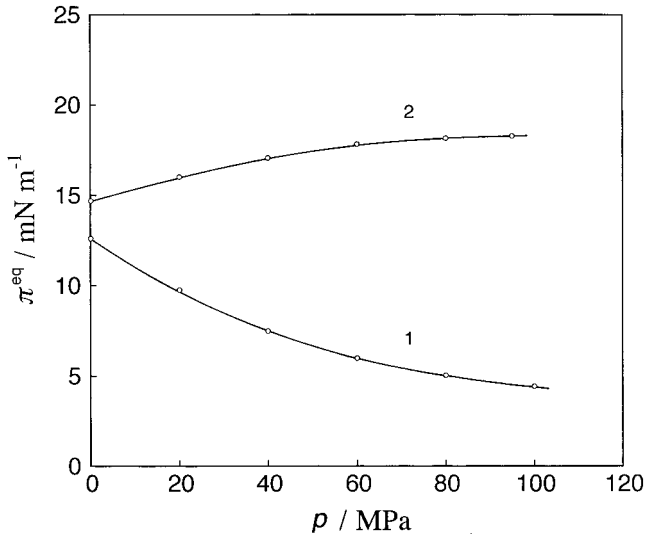

Figure 10. Transition pressure vs pressure curves: (1) expanded−condensed transition, (2) $FC_{10}OH$ condensed−$C_{20}OH$ condensed transition.

TABLE 1: Values of Coefficient of dp of Equation 19 at 0.1 MPa

first transition (expanded ↔ condensed)	
Δv^{e}	−0.036 mm^3 m^{-2}
Δv^{c}	−0.191
$\Gamma^{H,e}$	3.21 μmol m^{-2}
$\Gamma^{H,c}$	5.14
Coeff. of dp	−0.198 mm^3 m^{-2}
second transition (FC condensed ↔ HC condensed)	
Δv^{Fc}	−0.190 mm^3 m^{-2}
Δv^{Hc}	−0.247
$\Gamma^{H,Fc}$	5.32 μmol m^{-2}
$\Gamma^{H,Hc}$	7.71
Coeff. of dp	0.088 mm^3 m^{-2}

in Figure 10. Let us briefly consider the pressure dependence of π^{eq} thermodynamically by employing the equation similar to eq 15. Since the total differential of γ^0 of the pure hexane/water interface is written by

$$d\gamma^0 = -\Delta s^0 dT + \Delta v^0 d\,p \quad (17)$$

where Δs^0 and Δv^0 are the entropy and volume of interface formation, respectively, the total differential of interfacial pressure π is given from eqs 3 and 17 by

$$d\pi = -(\Delta s^0 - \Delta s)dT + (\Delta v^0 - \Delta v)d\,p + \Gamma^{H}(RT/m)dm + \Gamma^{H}(RT/X_1X_2)(X_2^{H} - X_2)dX_2 \quad (18)$$

Then the total differential of π^{eq} is given by

$$d\pi^{eq} = -\{[(\Delta s^0 - \Delta s^{\alpha})/\Gamma^{H,\alpha} - (\Delta s^0 - \Delta s^{\beta})/\Gamma^{H,\beta}]/(1/\Gamma^{H,\alpha} - 1/\Gamma^{H,\beta})\}dT + \{[(\Delta v^0 - \Delta v^{\alpha})/\Gamma^{H,\alpha} - (\Delta v^0 - \Delta v^{\beta})/\Gamma^{H,\beta}]/(1/\Gamma^{H,\alpha} - 1/\Gamma^{H,\beta})\}d\,p + (RT/X_1X_2)[(X_2^{H,\alpha} - X_2^{H,\beta})/(1/\Gamma^{H,\alpha} - 1/\Gamma^{H,\beta})]dX_2 \quad (19)$$

Therefore, it is realized that the pressure dependence of π^{eq} is closely related to the partial molar volume change of adsorption at the phase transition points. The coefficients of dp of eq 19 were evaluated for the first and second transition at 0.1 and 80 MPa, and the results are shown in Tables 1 and 2, respectively,

TABLE 2: Values of Coefficient of dp of Equation 19 at 80 MPa

first transition (expanded ↔ condensed)	
$\Delta\nu^{e}$	0.005 mm^3 m^{-2}
$\Delta\nu^{c}$	−0.141
$\Gamma^{H,e}$	1.65 μmol m^{-2}
$\Gamma^{H,c}$	5.54
Coeff. of dp	−0.043 mm^3 m^{-2}
second transition (FC condensed ↔ HC condensed)	
$\Delta\nu^{Fc}$	−0.155 mm^3 m^{-2}
$\Delta\nu^{Hc}$	−0.231
$\Gamma^{H,Fc}$	5.66 μmol m^{-2}
$\Gamma^{H,Hc}$	8.17
Coeff. of dp	0.008 mm^3 m^{-2}

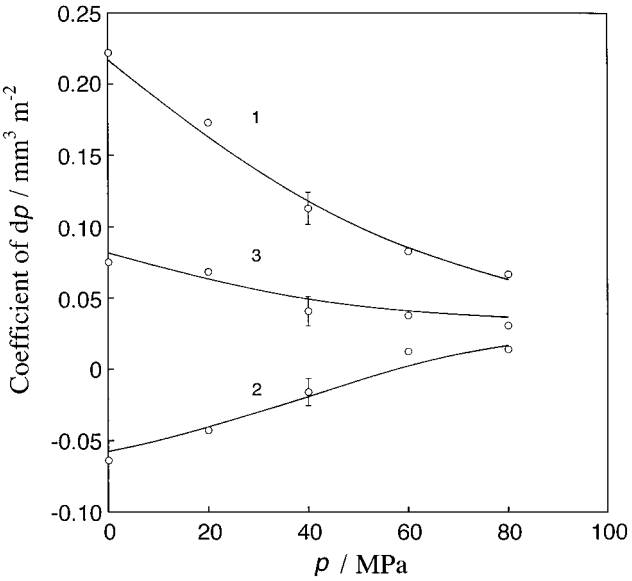

Figure 11. Values of coefficient of dp of eqs 14 and 20 vs pressure curves: (○) eq 14, (—) eq 20; (1) expanded−condensed transition, (2) $FC_{10}OH$ condensed−$C_{20}OH$ condensed transition, (3) gaseous−expanded transition.

together with the $\Delta\nu$ and Γ^{H} values. It is noted that the coefficients of dp are negative for the first transition and positive for the second, respectively. This is consistent with the finding that the π^{eq} of the second break point increases and that of the first decreases with increasing pressure.

Finally, let us examine the order of phase transition found in this study. Since γ^{eq} is a function of T, p, and X_2, its differential form is written by

$$d\gamma^{eq} = (\partial\gamma^{eq}/\partial T)_{p,X_2}dT + (\partial\gamma^{eq}/\partial p)_{T,X_2}\,dp + (\partial\gamma^{eq}/\partial X_2)_{T,p}dX_2 \quad (20)$$

The coefficient of dp of eq 14 was calculated by using the $\Delta\nu$ and Γ^{H} values at the phase transition points, and that of eq 20 was evaluated from the slope of the γ^{eq} vs p curves shown in Figure 3. If the values of both coefficients evaluated separetely are in good agreement with each other, we can claim that the first-order phase transitions take place in the adsorbed film, i.e., there are break points on the γ vs p and m curves and therefore the $\Delta\nu$ and Γ^{H} change discontinuously at the points. This is one of the strategies to substantiate phase transition as well as those based on the surface equation of state such as Frumkin's formula.[25] In Figure 11 are compared both coefficients for the three types of phase transitions; the agreement is fairly good for the three kinds of the phase transitions and therefore the first-order phase transitions take place in the adsorbed film of $C_{20}OH$ and $FC_{10}OH$ mixture under high pressure.

Conclusion

The adsorption behavior of the $C_{20}OH$−$FC_{10}OH$ mixture employed in the previous study was investigated by means of the interfacial tension measurement by tuning pressure and concentration at $X_2 = 0.280$ and 298.15 K and analyzing the experimental results thermodynamically.

We obtained the following results.

(1) By drawing the interfacial pressure π vs mean area per molecule A curves at various pressures, it was found that the adsorbed film exhibits the three kinds of first-order phase transitions (gaseous−expanded, expanded−$FC_{10}OH$ condensed, and $FC_{10}OH$ condensed−$C_{20}OH$ condensed). This finding totally supports our previous conclusion on the phase transition.

(2) The difference in the pressure dependence of the partial molar volume change, $\bar{v}_i^{H} - v_i^{O}$, between the two kinds of condensed states led to the inference that the pressure dependence of the partial molar volume is in the order of $|\partial v_2^{O}/\partial p| > |\partial v_1^{O}/\partial p| > |\partial \bar{v}_2^{H}/\partial p| \approx |\partial \bar{v}_1^{H}/\partial p|$.

(3) The pressure coefficient of transition pressure π^{eq} was calculated by using the $\Delta\nu$ and Γ^{H} values at the transition points and found to be negative for the expanded−$FC_{10}OH$ condensed transition and positive for the $FC_{10}OH$ condensed−$C_{20}OH$ condensed transition. This result was consistent with our finding that the π^{eq} value of the former transition increases and that of the latter decreases with increasing pressure.

Acknowledgment. This work was supported in part by the Grant-in-Aid for Encouragement of Young Scientists of The Ministry of Education, Science, Sports and Culture (No. 10740326) and in part by the Kurata foundation.

References and Notes

(1) Hönig, D.; Möbius D. *J. Phys. Chem.* **1991**, *95*, 4590.
(2) Hénon, S.; Meunier, J. *Rev. Sci. Instrum.* **1991**, *62*, 936.
(3) Brezesinski, G.; Scalas, E.; Struth, B.; Möhwald, H.; Bringezu, F.; Gehlert, U.; Weidemann, G.; Vollhardt, D. *J. Phys. Chem.* **1995**, *99*, 8758.
(4) Kahlweit, M.; Strey, R. *Angew. Chem., Int. Ed. Engl.* **1985**, *24*, 654.
(5) Hutchinson, E. *J. Colloid Sci.* **1948**, *3*, 219.
(6) Jasper, J. J.; Houseman, B. L. *J. Phys. Chem.* **1965**, *69*, 310.
(7) Lutton, E. S.; Stauffer, C. E.; Martin, J. B.; Fehl, A. J. *J. Colloid Interface Sci.* **1969**, *30*, 283.
(8) Aveyard, R.; Briscoe, B. J. *J. Chem. Soc., Faraday Trans. 1* **1972**, *68*, 478.
(9) Lin, M.; Firpo, J. L.; Mansoura, P.; Baret, J. F. *J. Chem. Phys.* **1979**, *30*, 2202.
(10) Matubayasi, N.; Motomura, K.; Aratono, M.; Matuura, R. *Bull. Chem. Soc. Jpn.* **1978**, *51*, 2800.
(11) Motomura, K.; Matubayasi, N.; Aratono, M.; Matuura, R. *J. Colloid Interface Sci.* **1978**, *64*, 356.
(12) Ikenaga, T.; Matubayasi, N.; Aratono, M.; Motomura, K.; Matuura, R. *Bull. Chem. Soc. Jpn.* **1980**, *53*, 653.
(13) Iyota, H.; Aratono, M.; Yamanaka, M.; Motomura, K.; Matuura, R. *Bull. Chem. Soc. Jpn.* **1983**, *65*, 2402.
(14) Takiue, T.; Yanata, A.; Ikeda, N.; Motomura, K.; Aratono, M. *J. Phys. Chem.* **1996**, *100*, 13743.
(15) Takiue, T.; Yanata, A.; Ikeda, N.; Motomura, K.; Aratono, M. *J. Phys. Chem.* **1996**, *100*, 20122.
(16) Takiue, T.; Matsuo, T.; Ikeda, N.; Motomura, K.; Aratono, M. *J. Phys. Chem. B* **1998**, *102*, 4906.
(17) Padday, J. F. In *Surface and Colloid Science*; Matijevic, E., Ed.; Wiley: New York, 1969; Vol. 1, p 101.
(18) Matubayasi, N.; Motomura, K.; Kaneshina, S.; Nakamura, M.; Matuura, R. *Bull. Chem. Soc. Jpn.* **1977**, *50*, 523.
(19) Rotenberg, Y.; Boruvka, L.; Neumann, A. W. *J. Colloid Interface Sci.* **1983**, *93*, 169.
(20) Cheng, P.; Li, D.; Boruvka, L.; Rotenberg, Y.; Neumann, A. W. *Colloids Surf.* **1990**, *43*, 151.

(21) Ferrari, M.; Liggieri, F.; Ravera, F.; Amodio, C.; Miller, R. *J. Colloid Interface Sci.* **1997**, *186*, 40.
(22) Motomura, K.; Aratono, M. In *Mixed Surfactant Systems*; Ogino, K., Abe, M., Eds.; Mercel Dekker: New York, 1993; Vol. 46, p 99.
(23) Motomura, K. *J. Colloid Interface Sci.* **1978**, *64*, 348.
(24) Takiue, T.; Matsuo, T.; Ikeda, N.; Motomura, K.; Aratono, M. *J. Phys. Chem. B* **1998**, *102*, 5840.
(25) Frumkin, A. Z. *Z. Phys. Chem.* **1925**, *116*, 466.